

Identifying alterations at the bone-implant-interface of experimental joint replacement prostheses models by means of new ultrasonic measurement methods

Friedrich, Antonia

Master's thesis / Diplomski rad

2023

Degree Grantor / Ustanova koja je dodijelila akademski / stručni stupanj: **University of Split, School of Medicine / Sveučilište u Splitu, Medicinski fakultet**

Permanent link / Trajna poveznica: <https://um.nsk.hr/um:nbn:hr:171:733444>

Rights / Prava: [In copyright](#) / [Zaštićeno autorskim pravom.](#)

Download date / Datum preuzimanja: **2024-05-20**



Repository / Repozitorij:

[MEFST Repository](#)



UNIVERSITY OF SPLIT



**UNIVERSITY OF SPLIT
SCHOOL OF MEDICINE**

Antonia Friedrich

**IDENTIFYING ALTERATIONS AT THE BONE-IMPLANT-INTERFACE OF
EXPERIMENTAL JOINT REPLACEMENT PROSTHESES MODELS BY MEANS OF
NEW ULTRASONIC MEASUREMENT METHODS**

Diploma thesis

**Academic year:
2022/2023**

**Mentor:
Prof. Dr. Johannes Brachmann**

Coburg, August 2023

Contents

Acknowledgement	v
1 INTRODUCTION	1
1.1 Significance of joint replacements	2
1.2 Anatomy of a joint	3
1.3 Fundamentals of joint replacement prostheses and surgical installation	5
1.4 Causes of prosthesis loosening	10
1.5 Diagnosis of prosthesis loosening	11
1.6 Approach to new diagnostic methods	12
2 OBJECTIVES	13
2.1 Aim of the study	14
2.2 Hypothesis	14
3 MATERIALS AND METHODS	15
3.1 Design and description of the research	16
3.2 Physical background	16
3.2.1 Principles of Acoustic Wave Behavior in Solids and Liquids . .	17
3.3 Determination of bone-implant distance	18
3.3.1 Necessity of a theoretical model	18
3.3.2 Development of a theoretical model	18
3.4 Experimental setup	20
3.5 Ethical approval	21
4 RESULTS	23
4.1 Validation test of the experimental approach	24
4.1.1 Cylindrical system (aluminium-water-aluminium)	24
4.1.2 Planar system (bone-water-metal)	26
4.1.3 Comparison of both systems	29
4.2 Bone-implant system	30

5	DISCUSSION	35
6	CONCLUSION	39
7	REFERENCES	41
8	SUMMARY	47
9	CROATIAN SUMMARY	51
10	CURRICULUM VITAE	55

Acknowledgement

I would like to express my sincere gratitude to my mentor Prof. Dr. Johannes Brachmann as well as my co-mentor Dr. Alexander Franck, who supported me from the beginning of the development of this idea until the final touch of this thesis.

I also want to thank Jan Lützelberger and Prof. Dr. Klaus Stefan Drese from the Institute of Sensor and Actuator Technology in Coburg for turning our shared vision into reality with their physical expertise and experimental skills.

A big thank you goes to my family, Alexander, Silke, Jonathan and Emilia, who always support me and believe in my goals as much as in my success.

And thank you to my boyfriend, Max, who made it all possible by constantly encouraging me and never doubting my capabilities even when I was.

Finally, I would like to thank all my friends who accompanied me on my way and without who I would not be who or where I am today.

1 INTRODUCTION

1.1 Significance of joint replacements

In recent years, the field of orthopedics and traumatology has witnessed a surge in joint replacement operations, attributed to the demographic shift towards an aging population and a more active elderly community ^(1,2). Among the most frequently performed surgeries in this domain, joint prosthetic operations have gained prominence ^(3,4). However, complications can arise years after the initial surgery, often necessitating the ultimate revision and replacement of the endoprosthesis ^(5,4). One such complication is the loosening of the implant within the bone, a phenomenon that can be attributed to either septic or aseptic factors ⁽⁶⁾.

The loosening of the implant, whether due to infection-induced biofilm formation (septic) or wear and tear (aseptic), presents a significant challenge in orthopedics. The ability to diagnose this loosening early is crucial for effective therapeutic intervention, which often involves timely replacement ⁽⁵⁾. Conventional diagnostic tools, such as computer tomographic (CT) scans, X-Ray imaging and magnetic resonance imaging (MRI), have limitations in terms of resolution, only being able to identify gaps from a certain size threshold ⁽⁷⁾.

Distinguishing between septic and aseptic loosening is paramount in choosing the appropriate treatment strategy ⁽⁸⁾. Clinical examination, radiological imaging, and laboratory blood work constitute the standard diagnostic approach ⁽⁹⁾. However, radiological methods, while prevalent, have downsides like radiation exposure and limited resolution. Furthermore, identifying biofilm through radiological techniques is typically a late-stage indication, coinciding with severe joint pain ⁽¹⁰⁾. Treatment of these loosened joint prostheses is usually a revision surgery in which the implant has to be replaced by a new one in another major surgery ⁽⁵⁾. This could be avoided if the diagnosis could be made in an earlier stage and preventive measures initiated. Therefore, it is important to find a way of identifying even small gaps at the bone-implant-interface in artificial joints as soon as possible while not harming the patient with invasive procedures or radiation as in classical X-Ray imaging or CT scans. The best way to do this would be through a noninvasive ultrasonic medical device that can check the status of any prosthetic joint quickly and harmlessly to the patient.

In our experimental research we intend to introduce a new way of checking artificial joints by non-invasively putting ultrasonic sensors on two sides of the joint. With this device we will be able to identify any changes that might occur between the prosthesis and the bone of the patient, as for example a loosening which leads

to gap formation at the bone-implant-interface.

1.2 Anatomy of a joint

As a reference for the description of basic anatomical features, the Atlas of Human Anatomy from author Frank H. Netter edition 8 of 2022 ⁽¹¹⁾ and the anatomy book Clinically Oriented Anatomy by Keith L. Moore edition 8 from 2017 ⁽¹²⁾ should be considered, unless otherwise indicated.

The human bone is a living tissue that continuously grows, regenerates and adapts to the demands of the body. The femur, also known as the thigh bone or femoral bone, is an excellent example of the complex structure and nature of bone tissue.

Figure 1.1 shows schematically the proximal part of the femoral bone. The femoral bone consists of an outer compact layer of bone known as the compacta or cortical layer, and an inner spongy area known as the cancellous bone or trabecular bone. The bone matrix, which makes up the bulk of bone, is composed of collagen fibers embedded in a mineralized ground substance. This matrix gives the bone its strength and elasticity.

The compact bone layer of the femur is divided into small units called osteons

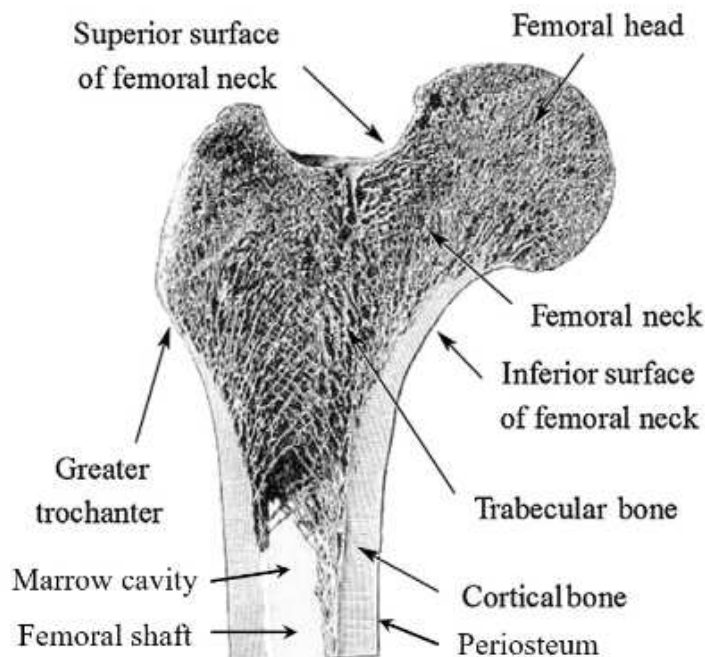


Figure 1.1: Schematic presentation of the anatomy of a femoral head ⁽¹³⁾.

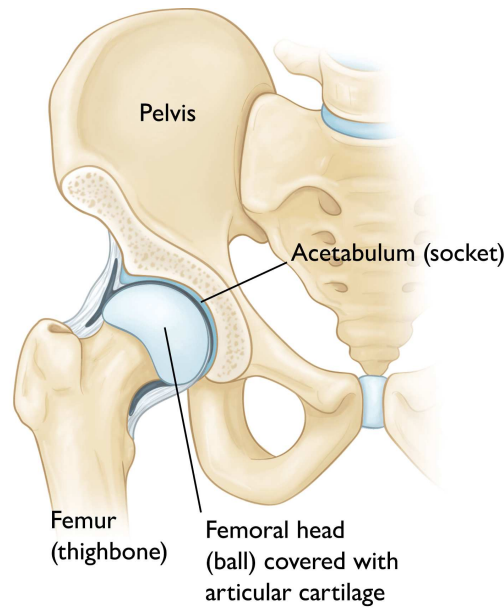


Figure 1.2: The human hip joint with its involved bony and cartilaginous structures.⁽¹⁴⁾.

or Haversian systems. Each osteon consists of concentric lamellae arranged around a central Haversian canal. These channels contain blood vessels and nerves that provide nutrients and communicate with the bone cells, known as osteocytes.

Inside the femoral bone, the cancellous bone forms a crosslinking structure of thin bone tubercles called trabeculae. This structure provides stability without adding unnecessary weight to the bone. The trabeculae are arranged so that they are aligned along the vertical lines in the bone, which optimizes load-bearing capacity.

The femoral bone also contains red bone marrow, which is responsible for the production of blood cells. The cavities of the cancellous bone contain stem cells that can develop into different types of blood cells, including red blood cells, white blood cells and platelets.

Mineralization is a crucial aspect of bone structure. Bones are composed of about two-thirds inorganic minerals, mainly calcium and phosphate. These minerals are deposited in the collagen matrix and give bone its rigidity and strength. Bones are dynamic body tissues and undergo constant remodelling, also called bone metabolism. This is a lifelong process in which new bone tissue is constantly formed by osteoblasts (ossification or new bone formation) and mature bone tissue is removed from the skeleton by osteoclasts which break down the old bone tissue (bone resorption). This process allows bone to adapt to stress and changes in the body.

In future references, the hip joint, shown in figure 1.2, will be our example to discuss the relevance of the ultrasonic measurement methods which can be transferred to any human joint.

The hip joint, also called the coxal or femoroacetabular joint, is a synovial ball and socket joint that connects the thigh bone (femur) and the pelvic bone (Os coxae). It is one of the biggest joints of the human body and allows a wide range of motion, including flexion, extension, abduction, adduction, internal rotation, and external rotation. The anatomical features of the hip joint include the femoral head (caput femoris), which is the round proximal part of the femur forming the ball of the joint. The surface of the femoral head is covered by smooth hyaline cartilage tissue that allows low-friction motion within the socket. The acetabulum is the shallow, cup-shaped depression in the pelvic bone into which the femoral head fits. The acetabulum is also lined with cartilage and, together with the femoral head, forms the ball and socket joint. A fibrocartilaginous ring, the labrum, surrounds the edge of the acetabulum. It deepens the socket and helps stabilize the hip joint. The joint capsule, a firm connective tissue envelope, surrounds and stabilizes the hip joint. It consists of strong ligaments that pull from the socket to the femoral head. The capsule contains synovial fluid that lubricates and nourishes the joint. The ligamentum capitis femoris connects the femoral head to the deep acetabulum. It has limited functional significance but contributes to the blood supply to the femoral head. The ligamentum teres femoris is a small ligament that extends from the femoral head to the deep acetabulum. It is also mainly used for stabilization and blood supply. A large number of muscles surround the hip joint and give it stability and mobility. These muscles include the hip flexors (for example the iliopsoas muscle), the hip extensors (gluteus maximus muscle), the hip adductors (adductor magnus, adductor longus, adductor brevis muscles), and the hip abductors (gluteus medius, gluteus minimus muscles).

The complex anatomy of the hip joint allows smooth motion and stability, which is critical for upright walking, running and other daily activities.

1.3 Fundamentals of joint replacement prostheses and surgical installation

Hip joint endoprotheses, or hip implants, have become a prevalent solution in orthopedic and traumatology procedures (¹⁵). The increasing incidence of coxarthroses

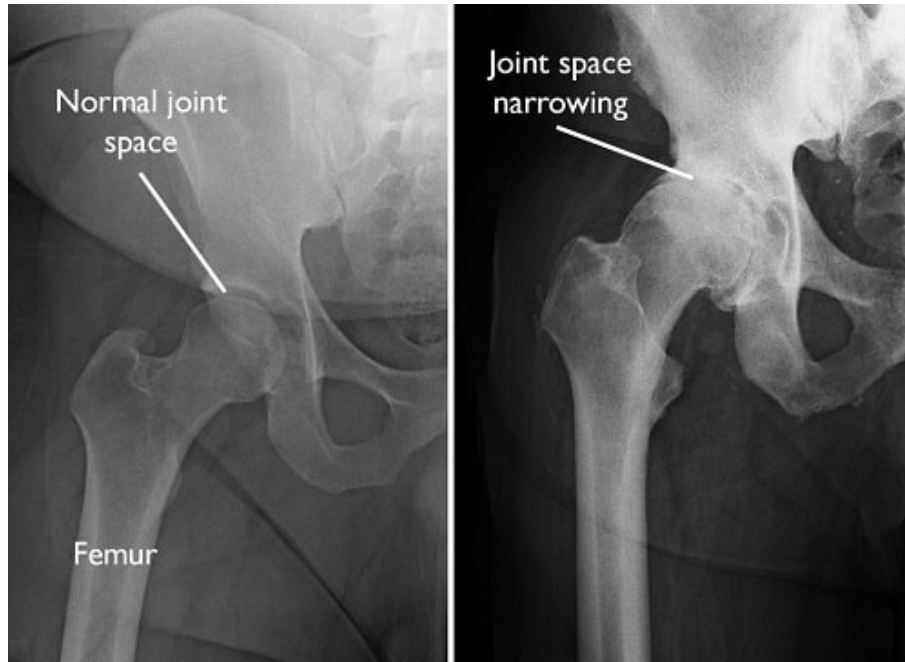


Figure 1.3: Comparison of a healthy joint with a normal joint space (left) and an arthritic hip joint with narrowed joint space (right). ⁽¹⁴⁾.

and femoral fractures in an aging population has driven the demand for these implants, making them the most common type of endoprosthetic procedure ⁽¹⁶⁾. A comparison of X-ray images of a healthy hip joint and one with coxarthrosis (figure 1.3) demonstrates the indication and necessity of a surgical joint replacement procedure.

In the field of orthopedics and traumatology, endoprosthetic surgeries have gained significant importance ⁽¹⁾. The surge in demand is driven by the growing prevalence of osteoarthritis, which is the most common indication for total hip arthroplasty ⁽¹⁶⁾. The remarkable advancements in medical technology have led to a wide range of various prosthetic materials, with a particular focus on metal stems used to anchor the implant securely within the femur ⁽⁴⁾.

Hip endoprotheses as shown in figure 1.4 embody multiple components that harmonize to replicate the natural structure and function of the hip joint. The femoral component is crafted from biocompatible metals like titanium or cobalt-chromium alloy ⁽¹⁸⁾. This component replaces the upper portion of the thighbone. Its stem is embedded firmly into the femur either with frictional force (cementless) or with the help of bone cement depending on the density and health of the patients femoral bone, ensuring stability and attachment to the bone ⁽¹⁹⁾. The acetabular component



Figure 1.4: Example of a hip endoprosthesis with a femoral stem (1), a femoral head (2), a plastic or ceramic liner (3, 4) and a acetabular socket (5).⁽¹⁷⁾.

is constructed from a blend of metal, ceramic, or plastic materials, this component replaces the hip socket. It provides a new articulating surface for the prosthetic femoral head, facilitating seamless movement. The femoral head within the acetabular component's socket is instrumental in facilitating joint motion. Materials such as metal, ceramic, or polyethylene dictate properties like wear resistance and friction reduction. Occasionally, a spacer made of medical-grade polyethylene is inserted between the femoral head and acetabular component to minimize friction and wear⁽⁴⁾. Various fixation techniques secure the firm attachment of the prosthesis to the existing bone. These can include cemented fixation, in which bone cement bonds the components, or uncemented fixation, in which new bone grows into the implant's surface over time⁽¹⁹⁾. The decision of the fixation method depends on the patient's bone, its density and overall condition. The femoral stem can be straight or possess various curves, adapting to the patient's anatomy and surgical approach⁽⁴⁾. It can also vary in length depending on the bone's structure, the bone's condition and potential fracture characteristics. Some implants offer liner options for the acetabular component, presenting choices for articulating surfaces.



Figure 1.5: X ray of an implanted hip endoprosthesis with displayed acetabular cup (1), femoral stem (2), cortical bone layer (3) and bone marrow cavity (4). ⁽¹⁷⁾.

Options encompass metal-on-metal, ceramic-on-ceramic, ceramic-on-polyethylene, or metal-on-polyethylene bearings ⁽²⁰⁾.

Surgical techniques of total hip arthroplasty include the posterior, lateral, and anterior approaches, each with its advantages based on patient needs ⁽²¹⁾. Similarly, cemented or cementless implantation is chosen based on bone density and the condition of the femoral bone. Future descriptions of surgical approach, technique and clinical outcomes will be based on the article of Stephen Petis Surgical approach in primary total hip arthroplasty: anatomy, technique and clinical outcomes ⁽²¹⁾.

Materials play a pivotal role in prosthetic design, ensuring durability, longevity, and biocompatibility. The ongoing refinement of materials drives progress in endoprosthetic surgeries, leading to improved patient outcomes and enhanced mobility.

This innovative field continually strives to perfect the harmony between human anatomy and medical technology.

Total hip arthroplasty (THA) surgery, also known as total hip replacement, is a surgical procedure performed on patients with severe hip joint damage due to osteoarthritis, injury or other pathological conditions indicating replacement of a joint. The procedure for THA surgery may vary slightly depending on the patient and medical facility, but generally follows the same general steps.

Prior to surgery, the patient undergoes a comprehensive medical evaluation to ensure that he or she is a suitable candidate for the procedure. This includes physical exams, blood tests, imaging, and cardiovascular evaluations, if necessary. The patient is given instructions on how to prepare for surgery, including dietary restriction and medication. THA surgery is usually performed under general anesthesia. The anesthesiologist will decide together with the patient on the appropriate method of anesthesia. The operating surgeon selects the access route to the hip. The most common access routes are the lateral approach, the posterior approach, and the anterior approach. Each approach has advantages and disadvantages in terms of visibility and soft tissue preservation. During the surgery, the surgeon removes the diseased or damaged joint tissue, including the damaged femoral head and acetabulum. Depending on the condition of the bone, partial removal of the femoral neck may also be necessary. After that, the surgeon inserts the prosthesis into the hip joint. The prosthesis consists of a metal alloy for the stem of the femur, an artificial femoral head, and a cup, often made of metal or plastic. The components are anchored into the bone.

The prosthesis can be fixed with or without bone cement. In the cemented procedure, bone cement is used to anchor the prosthetic components into the bone. In the cementless procedure, the bone grows directly into the prosthesis surface over the course of several weeks. After the prosthesis implant is securely positioned, the muscles and soft tissues are carefully reclosed to create a stable and protective environment for the prosthesis. The wound is sutured or closed with staples, and a sterile dressing is applied. After surgery, the patient is taken to the recovery room where his vital signs are monitored. The patient is then transferred to the hospital room where the recovery and rehabilitation phase begins. Early mobilization and physical therapy are critical to promote mobility of the new hip joint and strengthen muscles.

THA surgery has the potential to significantly improve the lives of patients with

hip joint damage by relieving pain and restoring mobility ⁽²²⁾. However, individualized consultation with the treating physician and thorough preparation are essential to achieve the best possible results.

1.4 Causes of prosthesis loosening

Loosening of arthroplasties, especially total hip arthroplasties (THA), is a serious complication that may require reoperation for correction. The causes of endoprosthesis loosening are varied and can be due to both mechanical and biological factors ⁽²⁴⁾.

Constant mechanical stress on the hip joint from movement and weight bearing can cause gradual breakdown of the bone around the implant over time. In this mechanical stress effect, the bone loses density due to reduced pressure under the implant. The resulting loosening can lead to instability of the prosthesis or trauma leading to periprosthetic fractures ⁽²⁵⁾. Despite advances in material technology, abrasion and wear can occur in the articulating surfaces of the prosthesis. Microscopic particles can be released and trigger an immune response in the body ⁽²⁶⁾. This can lead to bone loss and loosening of the prosthesis ⁽²⁶⁾. Infection in the

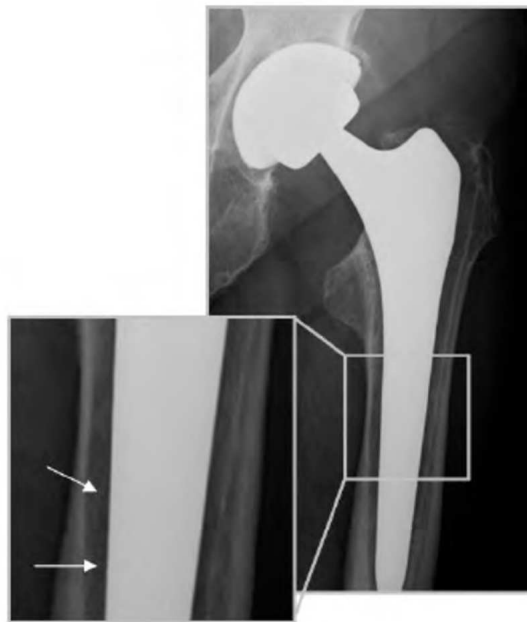


Figure 1.6: X ray of an implanted hip endoprosthesis with visible gap formation around the femoral stem of the prosthesis (arrows). ⁽²³⁾.

area of the implants, whether from a bacterial infection after surgery or from a subsequent infection in the body, can lead to loosening by formation of a biofilm at the bone-implant-interface ⁽²⁷⁾. Bacteria can form a biofilm that compromises the firm connection between the bone and the prosthesis ⁽²⁾. Incorrect implantation or improper positioning of the prosthesis during surgery can result in uneven loading, which can also ultimately lead to loosening. Furthermore, the quality of the surrounding bone plays always a crucial role. Osteoporosis or other bone diseases may affect the ability of the bone to hold the prosthesis stably. Also, some patients may have an immune reaction to the implants that leads to bone loss. Obesity and excessive physical activity can increase the stress on the prosthesis and accelerate wear. ⁽²⁸⁾

To prevent loosening of hip arthroplasties, careful planning, precise implantation, use of high-quality materials, and regular medical follow-up examinations are critical ⁽²⁹⁾. Research in this area is aimed at improving the long-term durability of arthroplasties and better understanding the factors that lead to loosening.

1.5 Diagnosis of prosthesis loosening

Diagnosis of prosthesis loosening, especially in total hip arthroplasty (THA), is a crucial step to take appropriate measures for treatment and correction in time. Various diagnostic approaches are used to identify the cause of loosening and select the best possible therapy ⁽³⁰⁾.

First and foremost, a thorough clinical examination by the orthopedic surgeon is the starting point. Symptoms such as pain, limited range of motion, instability and lameness indicate a possible complication of the implanted prosthesis. Imaging techniques play a key role in diagnosing prosthetic loosening. Standard radiographs provide an initial assessment. Loosening can be detected by visible gaps between the implant and bone or by changes in the course of the bone structures. Advanced imaging modalities such as CT scans or MRI can provide more detailed insight into prosthesis loosening, but all of these imaging measures are limited. ^(30,6) Early and accurate diagnosis is critical to determine the correct treatment strategy and minimize long-term complications.

1.6 Approach to new diagnostic methods

In our investigation by means of experiments on a model of human bone, ultrasonic measurement devices have established themselves as a promising and innovative diagnostic method, especially in the evaluation of gap widths between bone and implanted prosthesis. This method would offer a non-invasive and precise way to monitor the integration of implants in bone tissue and to detect potential loosening or complications at an early stage.

The use of ultrasound to determine gap widths between bone and prosthesis offers several advantages over conventional diagnostic methods. Ultrasound allows real-time imaging, which would enable clinicians to observe changes immediately. Moreover, the method is radiation-free, making it safer for patients and users compared to current standard imaging techniques such as X-ray or CT scans.

The technology of ultrasound is based on the evaluation of sound waves that are transmitted through the tissue and prosthesis. By analyzing the travel time, intensity and reflection of the sound waves, clinicians could draw precise conclusions about the structure and condition of the connection between the bone and the prosthesis. As a result, loosening, infection or other abnormalities at the bone-implant-interface could be detected early before they lead to serious problems.

The use of ultrasound to evaluate gap widths between bone and implanted prosthesis shows promising results that can improve patient care. Nevertheless, it is important to note that this technique is progressing in development and application, and further research and clinical studies are needed to validate its efficacy and accuracy.

2 OBJECTIVES

2.1 Aim of the study

This study aims to evaluate the feasibility of ultrasound as a non-invasive method to characterize bone to implant alterations and lead to the development of novel ultrasonic measurement devices capable of characterizing the interface between bone and implant in a clinical setting. We will discuss the questions if bone properties can be determined non-invasively using ultrasonic sensors and if the ingrowth of implants can be monitored quantitatively using ultrasound. This study is an experimental study using an artificial bone model that will be created resembling the structure of the human body. Our goal is to detect liquids in interfaces between bone and implant with the help of the intensity of microacoustic surface waves. Our goal is to exploit ultrasonic measuring to reliably identify gap dimensions ranging from 500 μ m to 2mm.

2.2 Hypothesis

Ultrasonic sensors allow identification of gaps at a much smaller size than conventional radiological methods and characterize the bone-implant-interface, thereby enabling early detection of aseptic or septic loosening of implanted endoprostheses.

3 MATERIALS AND METHODS

3.1 Design and description of the research

In the course of this project an idealized system has been used in order to validate the use of ultrasonic waves for measuring bone-prosthesis-distances. Thereby, human skin, fat and muscle tissue are neglected such that the ultrasonic waves are in direct contact to the bone. For a more thorough understanding Section 3.2 provides a brief review on the physical background of ultrasonic waves and its behavior in different materials. The determination of bone-prosthesis-distances is based on a mathematical model which is summarized in Section 3.3. For the calculation however, experimental ultrasonic spectra have been measured with the setup described in Section 3.4

3.2 Physical background

Unless otherwise stated, all physical and acoustic correlations are taken from the textbook by Lerch, which is also cited by Jan Lützelbergers bachelor thesis and the according article in the *sensors* journal which should be consulted for further insight into the physical details of this research (^{31, 32, 33}).

From a physical perspective, the interface between bone and implant to be examined by ultrasound represents a system with three layers. Externally, there is the solid cortical layer, also known as cortical bone. Below that is a fluid, demineralized layer that serves as an intermediate medium followed by the solid prosthetic stem. Sound waves are generated outside this system and, simplistically, are produced by a transducer on the cortical bone (³⁴).

In the real scenario, the clear delineation of the phases does not occur in this strict manner, as there is no clear, distinct interface. Instead, a transition region exists between the mineralized and demineralized regions. It is important to note that the system is actually composed of multiple layers. Nevertheless, a simplified representation as a three-layer system will be used for the time being in order to develop an ultrasonic-based measurement method that is suitable for the application. Before we deal with the actual experimental set up in Section 3.4, the basic physical principles of sound waves and their propagation will first be explained.

3.2.1 Principles of Acoustic Wave Behavior in Solids and Liquids

Acoustics is the scientific study of sound, encompassing the study of mechanical vibrations occurring within elastic mediums. These vibrations propagate through gases, liquids, and solids, undergoing processes such as reflection, refraction, diffraction, and interference. Sound is often categorized based on its frequency, denoted as f . The audible range for the human ear falls between approximately 20 Hz and 20 kHz, termed as auditory sound. Sound waves with lower frequencies are referred to as infrasound, while those with higher frequencies are known as ultrasound. The latter frequency range not only holds a critical role in medical imaging but also exclusively serves as the focal point for investigation within the context of this thesis.

Within the idealized three-layer-system the ultrasound waves travel through a liquid and two solid layers as depicted in Figure 3.1. Thereby, an initial ultrasound wave denoted as u_i is partially reflected denoted as u_{R_1} and u_{R_0} . The remaining waves are transmitted denoted as u_{T_0} and u_{T_2} . The ratio of reflection and transmission is described by the reflection coefficient which can then be obtained by experimental measurements.

Sound propagation in liquids

In gases and liquids, sound waves travel through the medium as periodic fluctuations in the fundamental variables: pressure, density, and particle velocity. These

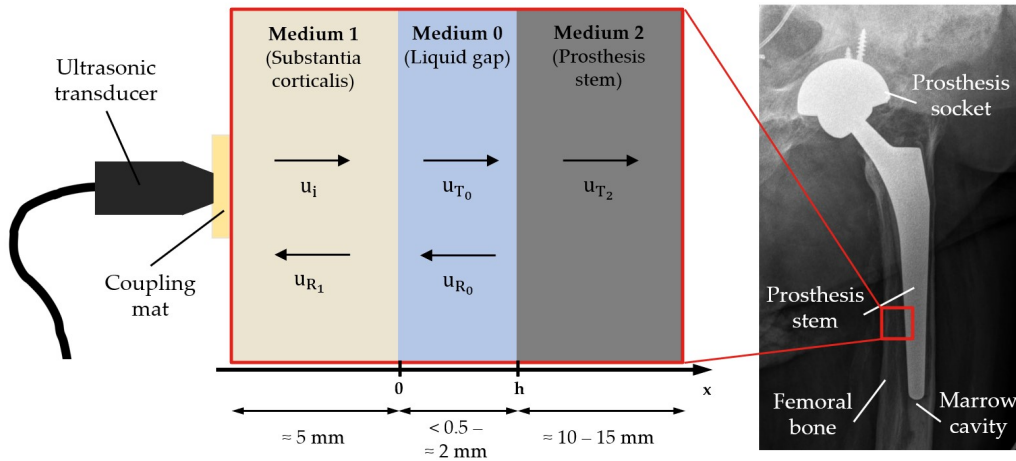


Figure 3.1: Schematic representation of the investigated three-layer-system. ⁽³¹⁾

deviations from the baseline values, induced by the propagating sound wave, are termed as sound pressure, sound density, and sound velocity. These quantities characterize the characteristics of the sound-occupied space, known as the sound field. As particles within liquid and gaseous substances lack the ability to transmit lateral forces, sound vibrations occur solely in the direction of propagation; these vibrations are classified as longitudinal waves.

Sound propagation in solids

Unlike liquids and gases, solids possess the capability to convey forces perpendicular to the propagation direction, owing to their molecular arrangement. This inherent trait results in these materials exhibiting elastic resistance not only to alterations in volume but also to modifications in shape. Specifically, when subjected to a change in shape alone, solids respond with opposing forces known as shear or thrust forces. As a consequence, in contrast to liquids and gases, a solitary constant is inadequate to fully depict the elastic characteristics of a solid body (such as a compressibility modulus or compression). For isotropic solids, like those featuring uniform properties in all directions, two constants become necessary (like elastic and shear moduli) to comprehensively describe their elastic behavior.

3.3 Determination of bone-implant distance

3.3.1 Necessity of a theoretical model

The measurements provide reflection coefficient data for the specified layers. To interpret these results, knowledge of the acoustic impedances of the materials and a theoretical model of the system are essential. The subsequent section introduces the conceptual foundation of this theoretical framework. For a comprehensive understanding, the reader is referred to the detailed exposition in the *sensors* paper ⁽³¹⁾.

3.3.2 Development of a theoretical model

In our simplified model, a three-layer system is considered, comprising cortical bone, a liquid intermediate layer, and a metallic implant. Notably, we exclude considerations of skin, fat tissue, and other soft tissues. Each of these layers ex-

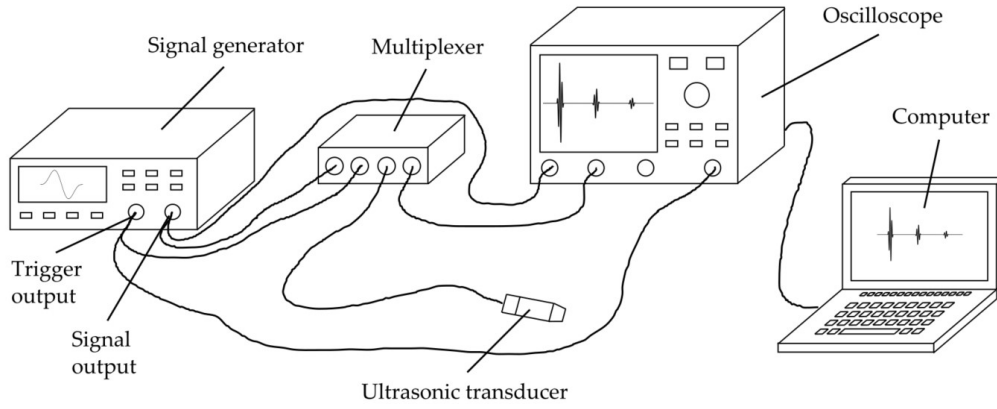


Figure 3.2: Schematic representation of the experimental setup for determining reflection coefficient spectra for a three-layer-system.

hibits distinct sound wave propagation behaviors due to their specific physical and chemical properties. Cortical bone, characterized by its mineral structure, behaves differently from the intermediate layer, which is anticipated to be liquid in nature, and the prosthesis with its metallic lattice structure. In liquids, sound waves propagate periodically, contingent upon the liquid's density, resulting in longitudinal waves. Conversely, in solids, sound waves travel through vibrations across their lattice structure, generating both longitudinal and transversal waves. However, due to the varying speeds of propagation for these two types of waves, they tend to separate. Consequently, our theoretical model simplifies the analysis by solely accounting for longitudinal waves.

When ultrasound transitions between layers, it triggers typical wave phenomena: reflection, interference, and dispersion. The wave experiences partial reflection and transmission (see Figure 3.1), where the proportion of reflection to transmission is once again dictated by the material's physical properties. Dispersive effects occur when the wave does not approach the layer perpendicularly. This leads to constructive and destructive interference, causing energy distribution of the original wave within the layer. This behavior manifests every time an ultrasound wave crosses layer boundaries. By possessing knowledge of the ultrasound frequency, speed of sound, and acoustic impedance of the bone structure, liquid intermediate layer, and metal, the thickness of the intermediate layer can be calculated.

3.4 Experimental setup

The measuring equipment used for the experiments, the totality of all measuring devices and additional equipment used, is shown schematically in Figure 3.2. The voltage signal required by the transducer (C 384-SU from Olympus) was generated by a function generator of type 33521A from Agilent Technologies. An amplitude of 10 V was used in burst mode with a burst period of 10 ms and a frequency of 3 MHz. The trigger and transmit signals were fed to a Teledyne LeCroy WaveRunner 604Zi digital oscilloscope and to a multiplexer. A 10:1 probe was used on the oscilloscope for the transmitted signal. The multiplexer, which was manufactured at the Institute of Sensor and Actuator Technology (ISAT) in Coburg, switched the transmit signal of the function generator through to the transducer on the rising edge of the trigger pulse and switched the transducer through to the oscilloscope on the falling edge. Through this electrical isolation of the function generator from transducer and oscilloscope during the receiving process we could ensure that the voltage measured at the oscilloscope, independent of the ohmic resistance of the

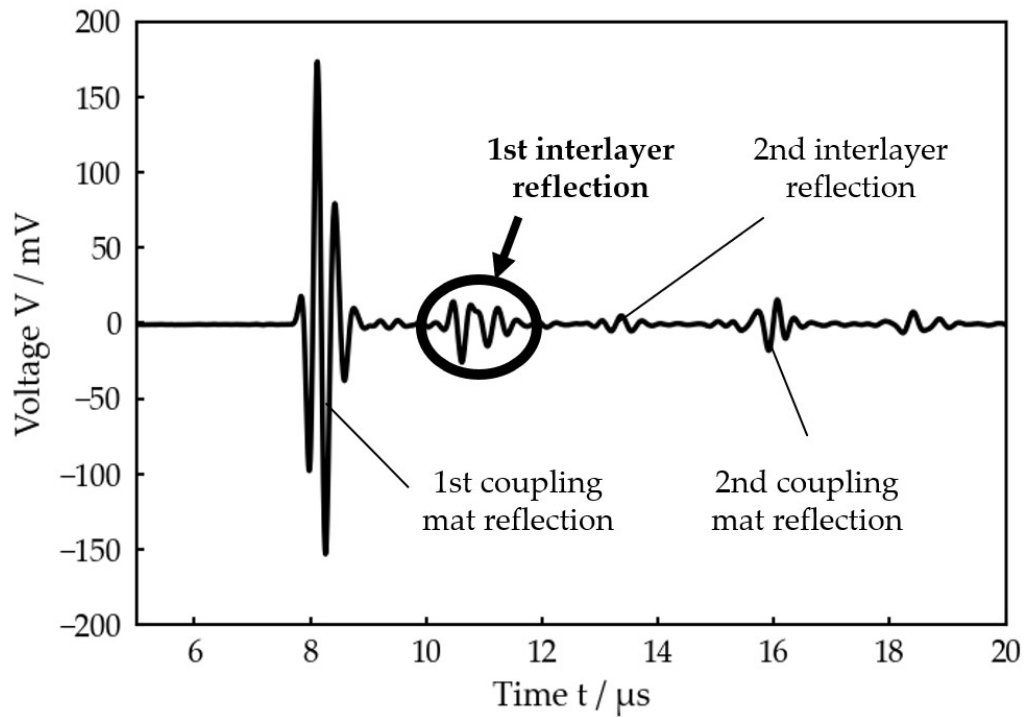


Figure 3.3: Schematic experimental spectrum as change in voltage over time. The first interlayer reflection is highlighted due to its importance for this study.

transducer, was the actual applied voltage. In addition, the received signal at the oscilloscope exhibited significantly greater stability. Transmit and receive signals were averaged 20-fold on the oscilloscope and filtered with a 2-bit digital noise filter. Subsequently, the voltage signals were transferred to a computer via the network interface of the oscilloscope using a measurement program developed at ISAT, where further data processing with the help of a developed algorithm for these ultrasonic wavelengths finally took place.

Making use of this experimental setup the ultrasonic transducer obtains a voltage signal as shown in Figure 3.3. For the purpose of determining the interlayer thickness only the first interlayer reflection has been used for the analysis with the developed mathematical algorithm.

3.5 Ethical approval

No ethical approval is needed for this study as all measurements are done on experimental models and any X ray or other diagnostic imaging pictures are disguised and any relation to patients details are unrecognizable.

4 RESULTS

4.1 Validation test of the experimental approach

Before performing measurements on a bone-implant setup, it was essential to carefully validate the theoretically developed measurement procedure. For this purpose, idealized test systems were used to ensure the accuracy and reliability of the procedure. Water served as an intermediate medium in these tests because its properties as density, sound velocity and sound impedance are similar to those of demineralized organic tissue types present in the human body. This similarity allowed a near realistic replication of the actual conditions in the human body. The first test systems, which were based on water, showed remarkable comparability with human body tissue. As a result, accurate test results could be obtained. These results were not only accurate but also transferable to the planned realistic implant setup. The validation thus created a reliable basis for the upcoming actual test, which was to investigate bone-implant interactions. These preparatory steps significantly minimized the risk and uncertainty in the actual testing procedure. Careful validation of the measurement procedure and the use of idealized test systems helped to ensure that the upcoming test on a bone-implant setup could be conducted on a profound and reliable basis.

4.1.1 Cylindrical system (aluminium-water-aluminium)

In order to test the feasibility of the developed measurement method, an ideal non-realistic experimental setup consisting of a planar aluminum-water-aluminum three layer system was selected. As this system is far from the actual clinical conditions in the human body, we decided on a more realistic shape of the first measurement set up with a cylindrical aluminium-water-aluminium three layer system as shown in Figure 4.1. This experimental setup consisted of an aluminum cone of 18 mm in diameter and a surrounding hollow cylinder. The hollow cylinder had external dimensions of 26 mm diameter and 4.5 mm wall thickness. The linear stage was used to set various layer thicknesses in intervals from 0 μm up to 1 mm.

The gap between the cone and the cylinder and thus the layer thickness was gradually reduced while ensuring with a syringe that the gap was always completely filled with water. At each set film thickness, one measurement was taken at a time using an oscilloscope and a measurement program. This was then evaluated on the computer and by applying the mathematical model the interlayer thickness was computed.

Table 4.1: Comparison of the set and calculated layer thickness for an idealized cylindrical aluminum-water-aluminum system.

layer thickness		layer thickness		layer thickness	
set	calc.	set	calc.	set	calc.
μm	μm	μm	μm	μm	μm
0	—	350	379	700	—
50	—	400	419	750	—
100	—	450	470	800	—
150	160	500	—	850	—
200	210	550	580	900	—
250	270	600	630	950	—
300	330	650	—	1000	—

Table 4.1 compares the experimentally set layer thicknesses to the calculated results and Figure 4.2 shows the measured and calculated spectrum for a layer thickness of 418 μm . With this set up, layer thicknesses in a range from 160 m to 630 m could be detected. For the other set values the separation of the coupling mat reflection and the first interlayer reflection (see Figure 4.2) in the obtained spectra was too small for further evaluation. Overall the calculated results are in good agreement with the largest deviation being in the range of 30 μm .

With this cylindrical three layer system it was possible to study the influence of curved surfaces that are shaped in a similar manner as the bone-implant interface

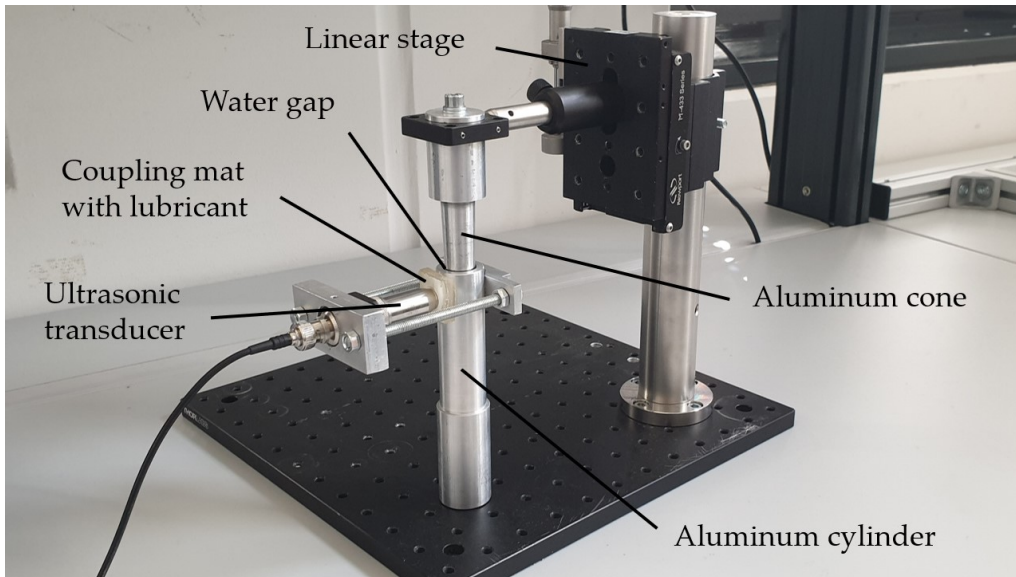


Figure 4.1: Experimental setup for a cylindrical aluminum-water-aluminum system. A linear stage was used to set the interlayer thickness (³¹).

in the human body. By simulating curved surfaces, measurable similarities to the natural structure of the bone-implant interface were established. Interactions and effects of ultrasonic sound propagation on these curved surfaces were analyzed.

4.1.2 Planar system (bone-water-metal)

A planar bone-water-titanium configuration was used next to explore the interactions between these materials in an idealized set up in more detail. Ideal geometric surfaces were chosen to provide a basis to start measurements. The materials, layer thicknesses and properties chosen helped to make the investigation as close to realistic conditions as possible while providing an ideal shape to perform measurements. The use of leaned and bleached water buffalo bone in a 4 mm thick plate allowed a well-controlled representation of the bone tissue. A 6 mm thick plate made of Titan-Aluminium-Vanadium alloy (Ti Al6 V4) provided the counterpart as model of an implant. This alloy is known for its biocompatibility and strength, which makes it a typically used material in cementless hip prosthesis stems. This specific set up aimed to analyze the interactions between bone, water and titanium. By realisti-

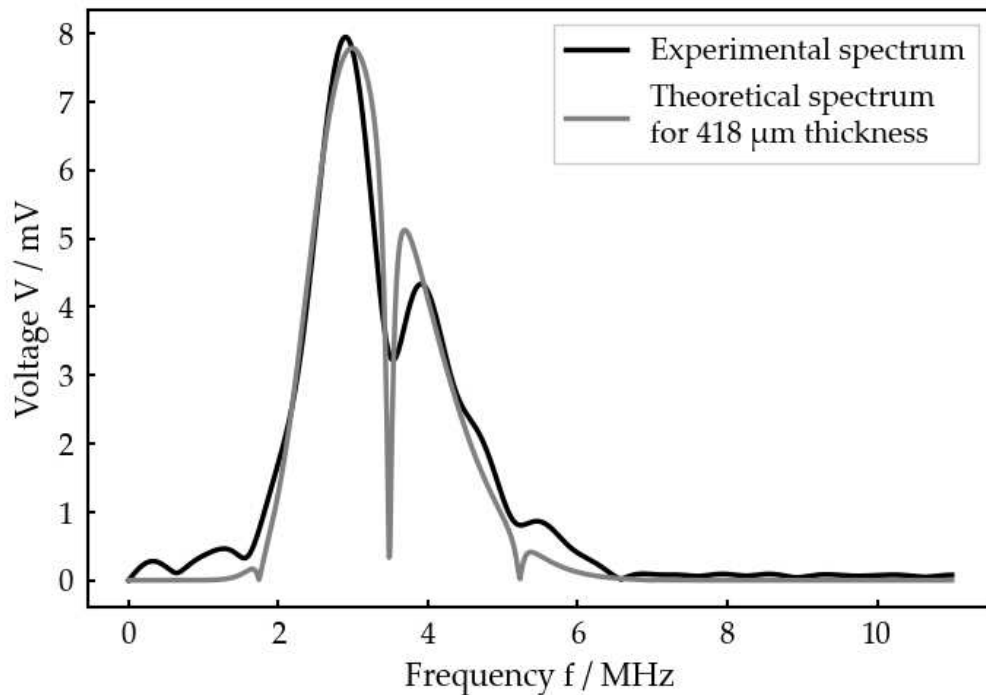


Figure 4.2: Ultrasonic spectrum for a cylindrical aluminum-water-aluminum system..

Table 4.2: Comparison of the set and calculated layer thickness for an idealized planar bone-water-titanium system.

layer thickness		layer thickness		layer thickness	
set	calc.	set	calc.	set	calc.
μm	μm	μm	μm	μm	μm
0	—	400	369	800	750
50	—	450	419	850	799
100	160	500	459	900	850
150	170	550	510	950	900
200	179	600	560	1000	940
250	219	650	610	1500	1429
300	270	700	650	2000	1919
350	320	750	700		

cally replicating materials and conditions, a better understanding of the potential interactions in implant environments could be gained. The experimental setup is shown in Figure 4.3.

Similar to the previous experimental procedure for the cylindrical system, the linear stage was used to set various layer thicknesses in the interval from 0 m to 2 mm and a measurement was carried out on each set thickness using an oscilloscope and measuring program. This was then again evaluated using an algorithm.

Table 4.2 compares the set layer thicknesses and the layer thicknesses determined

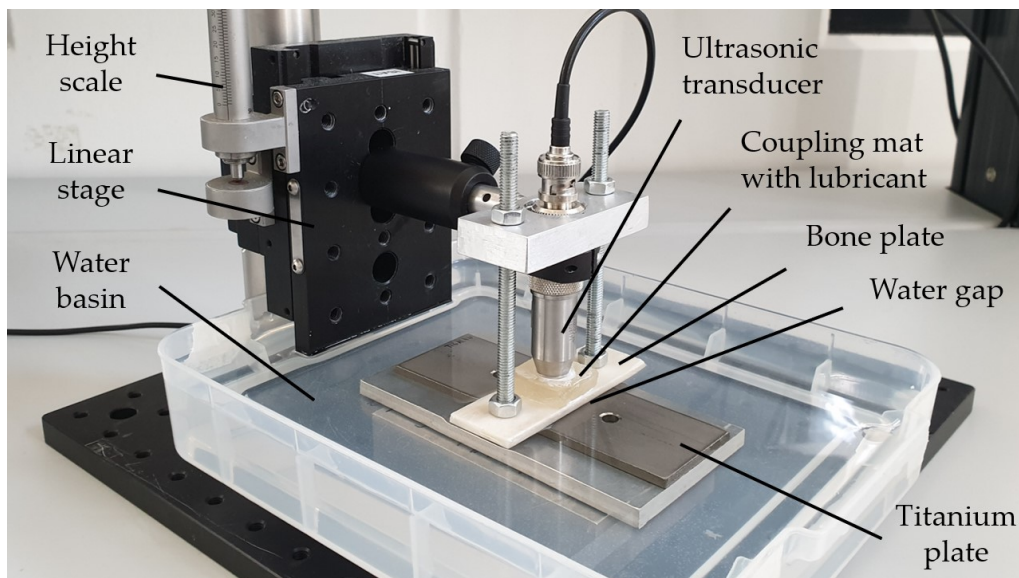


Figure 4.3: Experimental setup for a planar bone-water-titanium system. A linear stage was used to set the interlayer thickness (³¹).

by the algorithm. On the planar bone-water-titanium system, layer thicknesses in a range from 160 μm to 1919 μm could be detected.

For every set layer thickness, a spectrum showing frequency to voltage of the measured received signals at the interlayer was compared to the theoretically calculated spectrum at this layer thickness. As an example Figure shows the measured signal values for a layer thickness of 941 μm . This leads to the assumption that in an idealized system as this planar three layer system, ultrasonic quantification of layer thickness is feasible. It can also be clearly seen that experimental and theoretical spectra show a better correlation than for the previous used cylindrical aluminum system. Overall, the best results yet were obtained with the bone-water-titanium plate system, although this was not necessarily expected in advance due to the rougher surface of the bone plate and its stronger attenuation compared to aluminum.

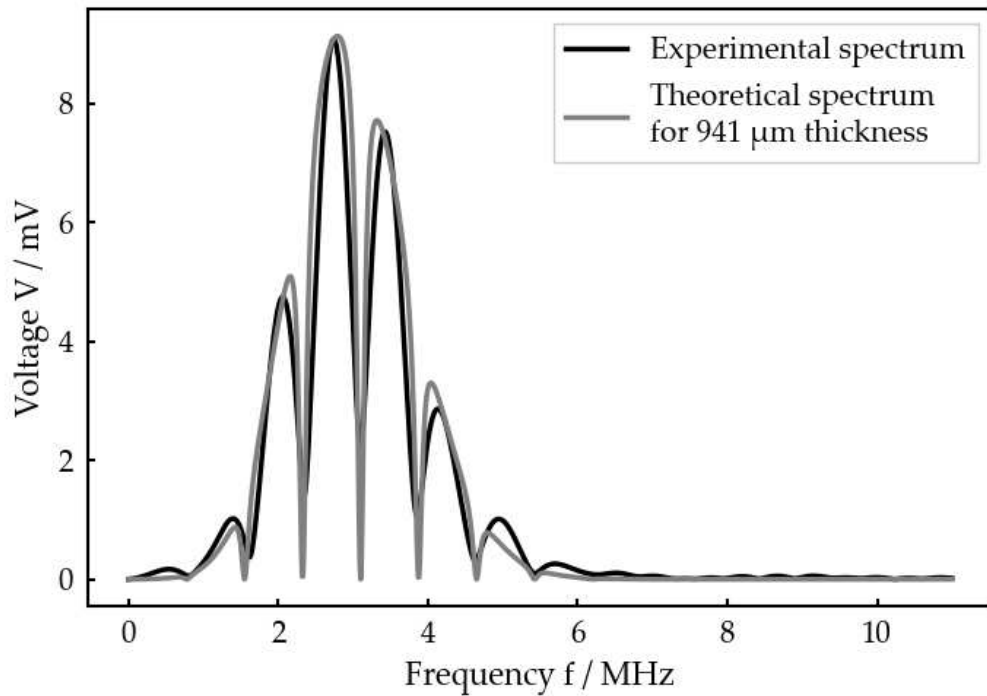


Figure 4.4: Ultrasonic spectrum for a planar bone-water-aluminum system.

4.1.3 Comparison of both systems

In both test setups, a linear stage was used to enable precise adjustment of the interlayer thickness. In the cylindrical setup, the varied interlayer thickness ranged from 0.0 to 1.0 mm, while in the planar setup the range was from 0.0 to 2.0 mm. Precise control of the interlayer thickness was crucial to understand the effects of variability on the interactions studied. Adjusting the parameters depending on the experimental setup allowed for a targeted investigation of different scenarios.

The results of the measurements are presented in Figure 4.5 and allow a comparison between the values obtained by the linear fitting of the thickness and the algorithmic calculation of both idealized systems. Figure 4.5 shows that our measurement method works well in these idealized conditions by demonstrating that calculated thickness and adjusted thickness for both systems are linearly related with a small slope error for the cylindrical as well as the planar system. Due to the linear correlation, a systematic error is inherent in the performed experiments. Moreover, the thicknesses in each series of measurements were subjected to linear fitting and the residuals were plotted against the adjusted thickness. The exceptionally low residual values, which were all below 10 m, confirm the precision of the measurements performed.

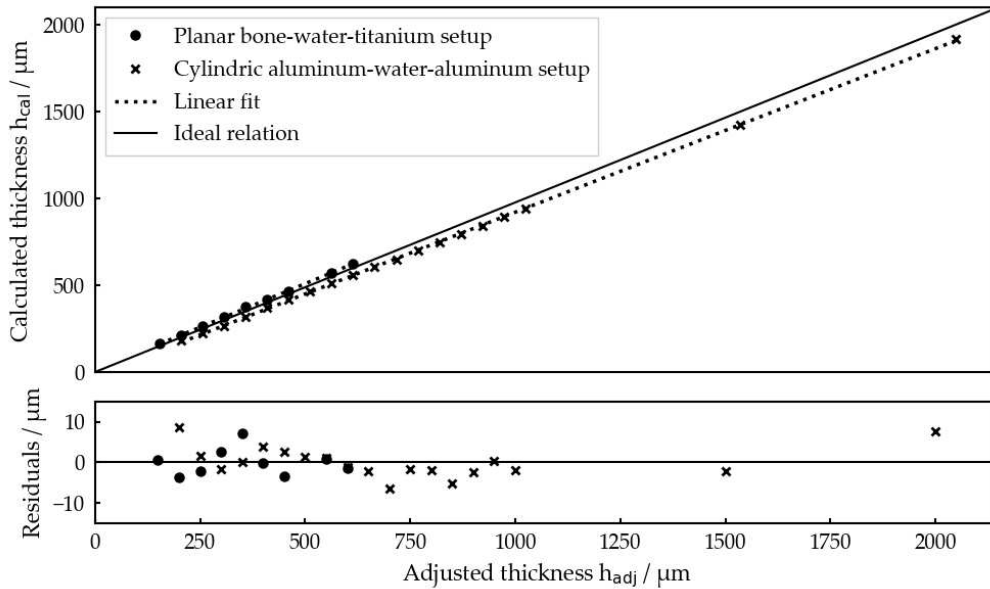


Figure 4.5: Correlation of calculated thickness and adjusted thickness for a planar and a cylindrical system.



Figure 4.6: Experimental setup for a realistic bone-water-implant system ⁽³¹⁾.

The analysis relied on mathematical equations that allowed a quantitative study of the interactions. The specific material properties were taken into account to obtain accurate results.

The suitability of the measurement method for curved surfaces was successfully demonstrated. The precise measurements performed on realistic materials and curved surfaces met the requirements for potential applications and confirmed the practical usefulness of the method.

4.2 Bone-implant system

Finally, the developed measurement method was to be tested on a clinically realistic bone-implant system, as far as this was feasible with the materials and equipment available. In this setup, a commercially available knuckle of pork was used as a substitute for the human femur. The knuckle was firstly boiled to remove the surrounding soft tissue. An acoustic transducer was attached to a relatively flat area of one of the tubular bones and fixated using a coupling mat greased with lubricant on both sides. The fixation was done by a fixture on the bone, for which the bone was partially mechanically processed.

A bone with a medullary cavity diameter of about 8-11 mm and a cortical bone thickness of about 2 mm was used for the measurements. The implant used was a hip prosthesis stem made of a cobalt-chromium-molybdenum alloy, which is used

in the clinical field especially but not exclusively for cemented hip prostheses. The bone and implant were placed in a pool of water, creating a continuous water gap between them. Variation of the thickness layers was achieved by manually inserting and removing the prosthesis stem. The experimental setup is shown in Figure (4.6).

A total of three measurement series were carried out. In the first series of measurements 14 individual measurements were performed while in the second and third series of measurements 15 individual measurements were performed in each case. The prosthesis stem was slowly pulled out of the medullary cavity manually, with the prosthesis stem fully inserted into the medullary cavity in the first measurement. Individual measurements were taken at regular intervals using an oscilloscope and a measurement program. The measurement data obtained were analyzed using the algorithm.

Table 4.3 summarizes the results for all three measurements showing that inter-layer thicknesses can be obtained by making use of the presented experiment.

In Figure 4.7 ,4.8 and 4.9 the experimental spectra of the interlayer reflection are presented in comparison with the theoretical spectrum and the corresponding specific layer thickness as an example of measurements carried out at different layer thicknesses.

The algorithm was able to determine layer thicknesses in all three series of measurements performed. In general, the layer thicknesses increase with increasing measurement number, except in measurement 4 of the third measurement series. The range of determined layer thicknesses extends from 210 μm to 1519 μm , thus covering almost the entire range from below 500 μm to about 2 mm. However, it is noted that accurate adjustment of smaller or larger thicknesses was not possible

Table 4.3: Computed layer thicknesses for a bone-water-implant-system. In total three measurements were performed in the range of 210 and 1596 μm .

measurement 1		measurement 2		measurement 3	
μm	μm	μm	μm	μm	μm
—	210	—	311	—	453
—	556	—	393	—	547
—	625	—	514	—	656
—	935	—	573	523	728
—	1255	—	852	—	797
—	1596	—	1016	—	854
—		—	1479	405	1510
—		—		443	

due to the lack of comparative measurements.

The comparisons between received signal and reflection spectrum showed significant differences between the different series of measurements. The shape of the reflection at the coupling mat in the first and third measurement series, as well as the interlayer reflection in the first measurement series, differed from the idealized test systems. Although the spectra exhibited stronger waves than those of the idealized setups, the spectral minima were clearly visible in the corresponding measurements.

The gained knowledge of these experimental set ups could be of great importance in implant research, as it can form the basis for optimizing implant design and performance.

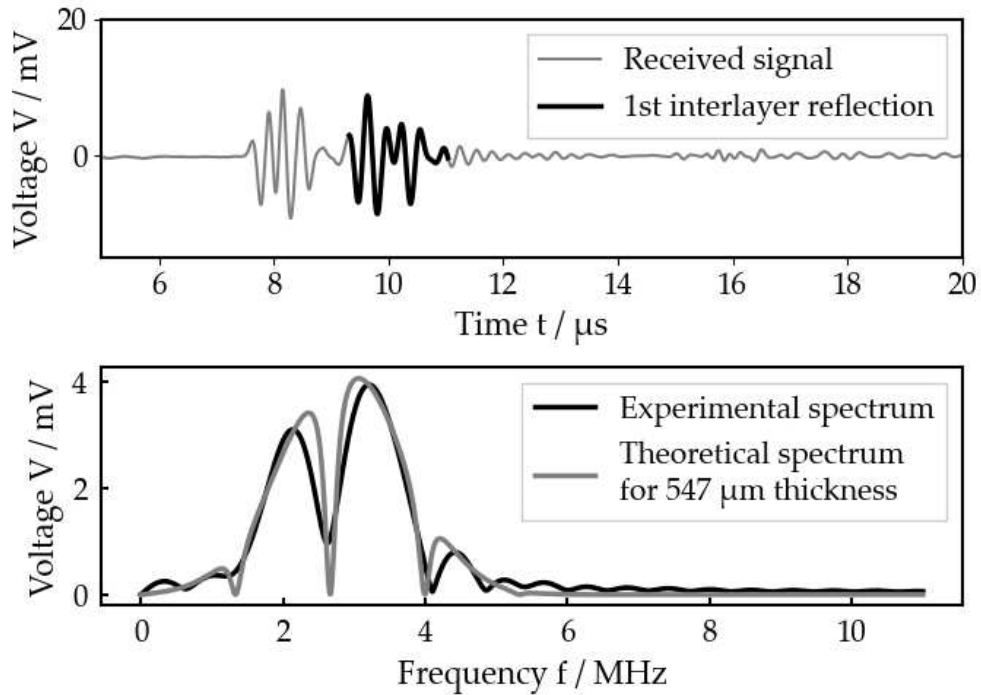


Figure 4.7: Measured and calculated ultrasonic spectrum for a hypothetical bone-implant system at 547 μ m.

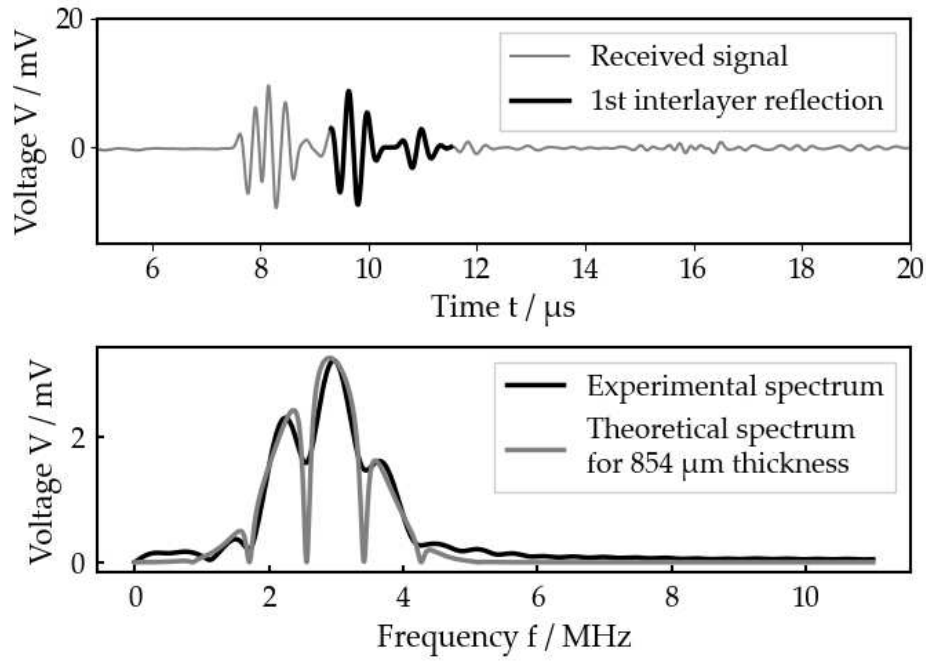


Figure 4.8: Measured and calculated ultrasonic spectrum for a hypothetical bone-implant system at 854 μm .

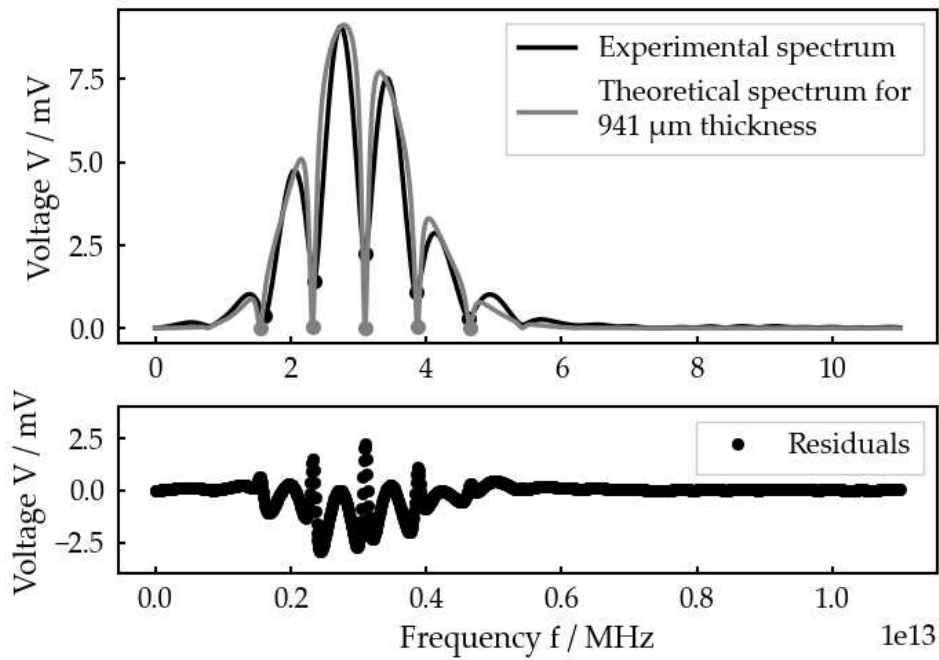


Figure 4.9: Measured and calculated ultrasonic spectrum for a hypothetical bone-implant system at 941 μm and the deviation of the experiment and the theoretical prediction is shown below in terms of the residuals.

5 DISCUSSION

The comparison of the experimental results on different test systems provided insights into the accuracy and reliability of the developed measurement method for determining the interlayer thickness. It was found that values for the thickness of the interlayer could be successfully determined in each setup, indicating the effectiveness of the applied method.

An expected observation was the tendency for the deviation between the set and determined layer thickness to increase as more realistic conditions were approached. This suggests that as the approximation to the real situation increases, the challenges in thickness determination increase, possibly due to more complex interactions or disturbances in the system.

Another finding was the possible reduction in the range over which the layer thickness determination could be made accurately. This suggests that it may be more difficult to obtain accurate thickness values under certain conditions, which could have important implications for the application of the technique. The increasing discrepancy between the experimental interlayer reflectance spectra and theoretical expectations was also notable. This could be due to several factors, including unexplained physical properties of the layer or unaccounted influences in the models.

Particularly surprising was the finding that the bone-water-titanium plate structure exhibited a significantly smaller deviation in terms of both layer thickness and reflectance spectrum. This suggests that this setup is particularly promising in terms of measurement accuracy and precision.

A remarkably small deviation between the adjusted and determined layer thicknesses was observed on the bone-water-titanium plate setup, indicating a high reliability of this setup. Similarly, there was an agreement between the experimentally obtained reflectance spectra and the theoretical predictions, underlining the significance of the results.

Particularly noteworthy was the fact that it was at the bone-water-titanium plate structure that the largest range for the precise determination of the layer thicknesses was found. This speaks to the versatility and great utility of this setup in the context of the measurement procedure developed. The results of this study suggest that the bone-water-titanium plate setup should be considered as the preferred choice for precise layer thickness measurements.

The main limitations when placing this experimental study in a future clinical field of application are clearly the approach of an idealized three layer system (planar or cylindrical) that would differ from a realistic scenario of a bone-implant system

in a clinical setting with soft tissues, muscles and skin. In our measurements of these idealized systems, slight errors and deviations occurred. This leads to the assumption that a real life application will lead to a larger magnitude error and thereby not fulfill the criteria to produce more reliable results than the current standard of X-Ray imaging.

Moreover, the characterized thickness of these three layer systems can only be calculated mathematically by an algorithm. To use this ultrasonic measurement method in a future clinical setting the algorithm has to be refined to ensure reliable results. However, adding more layers into the algorithm might require further approximations and thus a lack of validity for a broader range of measurements.

In order to achieve reproducible results in measurements one would assume that every bone in every human has the same characteristics with regard to its density (e.g. osteoporosis), shape and its surrounding tissues which is not the case.

The presented diagnostic tool made use of a specifically designed sensor in order to measure the ultrasonic waves. In order to apply this method clinically, such sensors need to be further tested, improved and produced on a large scale for clinical use.

6 CONCLUSION

This study's method to measure the bone-implant interface was effectively verified using two simplified test systems within a range spanning from 200 μm to 2 mm. This method was then extended to a more realistic bone-implant system encompassing distances between 200 μm and 1.6 mm. Furthermore, this technique demonstrated its suitability for heterogeneous, permeable materials featuring uneven surfaces, similar to those encountered in actual clinical bone-implant setups.

The results of our experimental study enable the possibility of similar measurements on a practical bone-implant system where bones are accompanied by soft tissues like fat, muscle, and skin. This comprehensive examination should include a comparative measurement aimed at assessing the precision of the gathered experimental data.

The algorithm employed could potentially facilitate characterizing the intermediate layer's properties and might find application in detecting the emergence of a biofilm. Further exploration, experimental assessment, and validation are warranted to substantiate this possibility.

Moreover, the enhancement of the analytical model and data processing methods should be pursued to minimize systematic inaccuracies effectively.

7 REFERENCES

- 1 Matharu G, Culliford D, Blom A. Projections for primary hip and knee replacement surgery up to the year 2060: an analysis based on data from The National Joint Registry for England, Wales, Northern Ireland and the Isle of Man. *Annals of the Royal College of Surgeons of England*. 2022 Jun;104:443-8.
- 2 Josse J, Valour F, Maali Y, Diot A, Batailler C, Ferry T, et al. Interaction Between Staphylococcal Biofilm and Bone: How Does the Presence of Biofilm Promote Prosthesis Loosening? *Frontiers in Microbiology*. 2019;10.
- 3 Taljanovic MS, Jones MD, Hunter TB, Benjamin JB, Ruth JT, Brown AW, et al. Joint Arthroplasties and Prostheses. *RadioGraphics*. 2003;23(5):1295-314. PMID: 12975517.
- 4 Slavković N, Vukašinović Z, Bašćarević Z, Vukmanović B. Total hip arthroplasty. *Srpski arhiv za celokupno lekarstvo*. 2012 07;140:379-84.
- 5 Weber M, Renkawitz T, Voellner F, Craiovan B, Greimel F, Worliceck M, et al. Revision Surgery in Total Joint Replacement Is Cost-Intensive. *BioMed Research International*. 2018;2018:8987104.
- 6 Sadoghi P, Liebensteiner M, Agreiter M, Leithner A, Böhler N, Labek G. Revision Surgery After Total Joint Arthroplasty: A Complication-Based Analysis Using Worldwide Arthroplasty Registers. *The Journal of Arthroplasty*. 2013;28(8):1329-32.
- 7 Burge AJ, Konin GP, Berkowitz JL, Lin B, Koff MF, Potter HG. What is the Diagnostic Accuracy of MRI for Component Loosening in THA? *Clinical Orthopaedics and Related Research*. 2019;477(9):.
- 8 Carlo L, Romanò D, Logoluso N, Meani E. Septic versus aseptic hip revision: how different? *Journal of Orthopaedics and Traumatology*. 2010;11(3):167-74.
- 9 Stotter C, von Roth P. Lockerungsdiagnostik in der Knieendoprothetik. *Der Orthopäde*. 2021;50(12):972-8.
- 10 Peel TN, Buising KL, Choong PF. Diagnosis and management of prosthetic joint infection. *Current Opinion in Infectious Diseases*. 2012;25(6):.
- 11 Netter FH. *Atlas of human anatomy*. vol. 8. Elsevier; 2022.

-
- 12 Moore KL. Clinically oriented anatomy. vol. 8. Lippincott Williams & Wilkins; 2017.
 - 13 Faisal TR, Luo Y. Study of stress variations in single-stance and sideways fall using image-based finite element analysis. *Bio-Medical Materials and Engineering*. 2016;27:1-14.
 - 14 Jared R H F. Osteoarthritis of the hip; [cited 25.08.2023]. Available from: <https://orthoinfo.aaos.org/en/diseases-conditions/osteoarthritis-of-the-hip/>.
 - 15 Ferguson RJ, Palmer AJ, Taylor A, Porter ML, Malchau H, Glyn-Jones S. Hip replacement. *The Lancet*. 2018;392(10158):1662-71.
 - 16 Cross M, Smith E, Hoy D, Nolte S, Ackerman I, Fransen M, et al. The global burden of hip and knee osteoarthritis: estimates from the Global Burden of Disease 2010 study. *Ann Rheum Dis*. 2014 Jul;73(7):1323.
 - 17 Rinio M. Hüftprothese: Vorteile, Haltbarkeit und Prothesenmodelle der künstlichen Hüfte; [cited 26.08.2023]. Available from: <https://gelenk-klinik.de/hueftoperation/hueftprothese/hueft-tep-kuenstliches-hueftgelenk.html>.
 - 18 Hu CY, Yoon TR. Recent updates for biomaterials used in total hip arthroplasty. *Biomaterials Research*. 2018;22(1):33.
 - 19 Hennrikus W, Pylawka T. Patellofemoral Instability in Skeletally Immature Athletes. *JBJS*. 2013;95(2):.
 - 20 Higuchi Y, Seki T, Hasegawa Y, Morita D, Komatsu D, Takegami Y, et al. Comparison of cementless total hip arthroplasty survivorship between metal-on-highly cross-linked polyethylene and ceramic on ceramic bearings: A case control study with a 5-9-year follow-up. *Orthopaedics & Traumatology: Surgery & Research*. 2018;104(5):663-9.
 - 21 Petis S, Howard JL, Lanting BL, Vasarhelyi EM. Surgical approach in primary total hip arthroplasty: anatomy, technique and clinical outcomes. *CAN J SURG*. 2015;58(2):128.
 - 22 Di Monaco M, Vallero F, Tappero R, Cavanna A. Rehabilitation after total hip arthroplasty: a systematic review of controlled trials on physical exercise programs. *Eur J Phys Rehabil Med*. 2009;45(3):303-17.

- 23 Ruther C, Timm U, Ewald H, Mittelmeier W, Bader R, Schmelter R, et al. Current Possibilities for Detection of Loosening of Total Hip Replacements and How Intelligent Implants Could Improve Diagnostic Accuracy; 2012. p. .
- 24 Varnum C. Outcomes of different bearings in total hip arthroplasty - implant survival, revision causes, and patient-reported outcome. *Dan Med J.* 2017;64(3):.
- 25 Akinbo O, Tyagi V. Acute Stress Fracture of the Pelvis after Total Hip Arthroplasty: A Case Report. *J Orthop Case Rep.* 2017;7(2):87-9.
- 26 Man K, Jiang LH, Foster R, Yang XB. Immunological Responses to Total Hip Arthroplasty; 2017.
- 27 Sebastian S, Malhotra R, Dhawan B. Prosthetic Joint Infection: A Major Threat to Successful Total Joint Arthroplasty. *Indian Journal of Medical Microbiology.* 2018;36(4):475-87.
- 28 Cherian JJ, Jauregui JJ, Banerjee S, Pierce T, Mont MA. What Host Factors Affect Aseptic Loosening After THA and TKA? *Clinical Orthopaedics and Related Research.* 2015;473(8):.
- 29 Apostu D, Lucaciu O, Berce C, Lucaciu D, Cosma D. Current methods of preventing aseptic loosening and improving osseointegration of titanium implants in cementless total hip arthroplasty: a review. *J Int Med Res.* 2017 Nov;46(6):2104-19.
- 30 Sandberg O, Carlsson S, Harbom E, Cappelen V, Tholén S, Olivecrona H, et al. Inducible displacement CT increases the diagnostic accuracy of aseptic loosening in primary total hip arthroplasty. *ActaO.* 2022;93:831-6.
- 31 Lützelberger J, Arneth P, Franck A, Drese KS. Ultrasonic Interferometric Procedure for Quantifying the Bone Implant Interface. *Sensors.* 2023;23(13).
- 32 Lützelberger J. Entwicklung eines Ultraschall-Messverfahrens zu Charakterisierung der Knochen-Implantat-Schnittstelle bei Hüftprothesen; 2022.
- 33 Lerch R, Sessler G, Wolf D. Technische Akustik. Heidelberg: Springer Vieweg; 2009.

-
- 34 Pithioux M, Lasaygues P, Chabrand P. An alternative ultrasonic method for measuring the elastic properties of cortical bone. *Journal of Biomechanics*. 2002;35(7):961-8.

8 SUMMARY

Objectives: This study aimed to evaluate the feasibility of ultrasound as a non-invasive method to characterize bone to implant alterations. Our goal was to show that ultrasonic sensors allow identification of gaps at a much smaller size than conventional radiological methods, thereby enabling early detection of loosened implanted endoprostheses.

Materials and methods: First, two idealized three layer systems, a cylindrical aluminium-water-aluminium system and a planar bone-water-metal system, were examined. Finally, the same measurements were carried out with a realistic three layer bone-water-implant system.

In all of these three layer system measurements a transducer (C 384-SU, Olympus) that generated ultrasonic signals controlled by a function generator (Agilent 33521A) was used. The transmitted signal was fed to an oscilloscope (Teledyne LeCroy WaveRunner 604Zi) and a multiplexer. The multiplexer, developed at the Institute of Sensor and Actuator Technology (ISAT), separated the transmit signal from the receive signal to ensure accurate voltage measurements. Finally, the signals were transmitted to a computer via a network interface for further processing.

Results: The measurement methods of this experimental study were applied to idealized test setups as well as a realistic bone-implant system.

Before performing tests on a bone-implant setup, the developed measurement procedure was secured by careful validation. Idealized test systems (a cylindrical three layer system composed of aluminium-water-aluminium and a planar three layer system composed of bone- water-metal) were used to ensure the accuracy and reliability of the procedure. Water was used as an intermediate medium as its properties are similar to those of demineralized tissue types in the human body. The water-based test systems showed remarkable comparability with human tissue, resulting in accurate results that were transferable to the realistic implant setup.

In the cylindrical setup, the varied interlayer thickness ranged from 0.0 to 1.0 mm, while in the planar setup the range was from 0.0 to 2.0 mm. A third more realistic system, a bone-implant system, was examined, in which the same measurements as with the previous two idealized systems were performed. The range of determined layer thicknesses extended from 210 μm to 1519 μm , thus covering almost the entire range from below 500 μm to about 2 mm.

The suitability of the measurement method for curved surfaces was successfully demonstrated. The precise measurements performed on realistic materials and curved surfaces met the requirements for potential applications and confirmed the

practical usefulness of the method.

Conclusion: The developed method for measuring the bone-implant interface was tested using simplified test systems in the range of 200 μm to 2 mm and then extended to more realistic bone-implant systems with distances from 200 μm to 1.6 mm. The method was also validated for heterogeneous permeable materials with uneven surfaces, as found in clinical bone-implant systems. The results allow similar measurements on practical bone-implant systems that include soft tissues such as fat, muscle, and skin. Future studies could use the algorithm to characterize interlayer properties and detect biofilm formation. Further improvements to the analytical model and data processing are needed to minimize systematic inaccuracies.

9 CROATIAN SUMMARY

Naslov: Identificiranje promjena na spoju kost-implantat eksperimentalnih modela nadomjesnih zglobnih proteza pomou novih ultrazvunih metoda mjerenja

Ciljevi: Ovo je istraivanje imalo za cilj procijeniti izvedivost ultrazvuka kao neinvazivne metode za karakterizaciju promjena kosti na implantatu. Na je cilj bio pokazati da ultrazvuni senzori omoguuju identifikaciju praznina puno manje veliine od konvencionalnih radiolokih metoda, ime se omoguuje rano otkrivanje olabavljenih ugraenih endoproteza.

Materijali i metode: Najprije su ispitana dva idealizirana troslojna sustava, cilindrični sustav aluminij-voda-aluminij i planarni sustav kost-voda-metal. Konano, ista su mjerenja provedena s realističnim troslojnim sustavom kost-voda-implantat.

U svim ovim mjerenjima troslojnog sustava koriten je pretvara (C 384-SU, Olympus) koji je generirao ultrazvune signale kojima upravlja funkcijski generator (Agilent 33521A). Odašlani signal je stavljen na osciloskop (Teledyne LeCroy WaveRunner 604Zi) i multiplekser. Multiplekser, razvijen na Institutu za tehnologiju senzora i aktuatora (ISAT), odvojio je prijenosni signal od prijemnog signala kako bi osigurao tona mjerenja napona. Na kraju su signali proslijeeni na raunalo putem mrenog suelja za daljnju obradu.

Rezultati: Metode mjerenja ove eksperimentalne studije primijenjene su na idealizirane ispitne postavke kao i na realističan sustav kosti i implantata. Prije izvoenja testova na postavu kotanog implantata, razvijeni postupak mjerenja osiguran je paljivom validacijom. Idealizirani testni sustavi (cilindrični troslojni sustav sastavljen od aluminij-voda-aluminij i planarni troslojni sustav sastavljen od kost-voda-metal) koriteni su kako bi se osigurala tonost i pouzdanost postupka. Voda je koritena kao meumedij jer su njezina svojstva slina onima demineraliziranih vrsta tkiva u ljudskom tijelu. Testni sustavi na bazi vode pokazali su izvanrednu usporedivost s ljudskim tkivom, to je rezultiralo tonim rezultatima koji su se mogli prenijeti na realističnu postavu implantata.

U cilindrinom postavu, različita debljina meusloja kretala se od 0,0 do 1,0 mm, dok je u planarnom postavu raspon bio od 0,0 do 2,0 mm. Ispitivan je tri realističniji sustav, sustav kost-implantat, u kojem su provedena ista mjerenja kao i kod prethodna dva idealizirana sustava. Raspon utvrenih debljina slojeva protezao se od 210 m do 1519 m, pokrivajući tako gotovo cijeli raspon od ispod 500 m do oko 2 mm. Uspjeno je dokazana prikladnost metode mjerenja za zakrivljene površine. Precizna mjerenja provedena na realnim materijalima i zakrivljenim površinama ispunila su zahtjeve za potencijalne primjene i potvrdila praktičnu korisnost metode.

Zakljuci: Razvijena metoda za mjerenje suelja kosti i implantata testirana je koritenjem pojednostavljenih testnih sustava u rasponu od 200 μm do 2 mm, a zatim proirena na realistinije sustave kosti i implantata s udaljenostima od 200 μm do 1,6 mm. Metoda je takoer potvrrena za heterogene propusne materijale s neravnim povrinama, kao to je pronaeno u klinikim sustavima kosti i implantata. Rezultati omoguuju slina mjerenja na praktinim sustavima kotanih implantata koji ukljuuju meka tkiva poput masti, miia i koe. Budue studije mogle bi koristiti algoritam za karakterizaciju svojstava meuslojeva i otkrivanje stvaranja biofilma. Potrebna su daljnja poboljanja analitikog modela i obrade podataka kako bi se sustavne netonosti svele na minimum.

10 CURRICULUM VITAE

General information

Name and surname: Antonia Friedrich
Date of birth: 22nd of May 1995
Place of birth: Kassel, Germany
Nationality: German
Address: Judengasse 43, 96450 Coburg, Germany
E mail: friedrich.antonina@gmx.net

Education

2017-2022 **University of Split** , School of Medicine
2013-2017 **Georg-August-Universität Göttingen**,
studies of chemistry and biochemistry
2005-2013 **Albert-Schweitzer-Schule Kassel**,
A levels

Work experience

January 2021 until present Working student at the department of orthopedics and traumatology,
REGIOMED Hospital Coburg
December 2020 - 2022 Covid-19 vaccination center, *Kassel*
July 2020 - December 2020 Intermediate care unit (nursing assistant),
REGIOMED Hospital Coburg
March 2017 - July 2017 Clinical traineeship in the hand surgical practice of Dr. Weißenborn, Kassel
August 2013 Clinical traineeship in the department of pediatrics,
Gesundheit Nordhessen Hospital Kassel
June 2012 - July 2012 Clinical traineeship in the department of obstetrics and gynecology,
Hospital Dr. Koch Kassel

Personal skills

Languages: German (native language)
English (C1 level)
French (B2 level)
Swedish (A1 level)